



HAL
open science

On the Ubiquity of Magnetic Reconnection Inside Flux Transfer Event-Like Structures at the Earth's Magnetopause

N. Fargette, B. Lavraud, M. Øieroset, T. Phan, S. Toledo-redondo, R. Kieokaew, C. Jacquey, S. Fuselier, K. Trattner, S. Petrinec, et al.

► **To cite this version:**

N. Fargette, B. Lavraud, M. Øieroset, T. Phan, S. Toledo-redondo, et al.. On the Ubiquity of Magnetic Reconnection Inside Flux Transfer Event-Like Structures at the Earth's Magnetopause. *Geophysical Research Letters*, 2020, 47 (6), 10.1029/2019GL086726 . hal-02886369

HAL Id: hal-02886369

<https://hal.science/hal-02886369>

Submitted on 15 Apr 2022

HAL is a multi-disciplinary open access archive for the deposit and dissemination of scientific research documents, whether they are published or not. The documents may come from teaching and research institutions in France or abroad, or from public or private research centers.

L'archive ouverte pluridisciplinaire **HAL**, est destinée au dépôt et à la diffusion de documents scientifiques de niveau recherche, publiés ou non, émanant des établissements d'enseignement et de recherche français ou étrangers, des laboratoires publics ou privés.

Copyright

Geophysical Research Letters

RESEARCH LETTER

10.1029/2019GL086726

Key Points:

- Nineteen percent of FTE-type structures observed by MMS during Phases 1A and 1B present signatures of magnetic reconnection in their core
- They seem to be formed by two magnetically disconnected interlaced flux tubes and are typically observed for large IMF B_y
- Several formation models are discussed, including a bifurcated X line scenario that results from the maximum shear angle model

Supporting Information:

- Supporting Information S1
- Table S1

Correspondence to:

N. Fargette,
nais.fargette@irap.omp.eu

Citation:

Fargette, N., Lavraud, B., Øieroset, M., Phan, T. D., Toledo-Redondo, S., Kieokaew, R., et al. (2020). On the ubiquity of magnetic reconnection inside flux transfer event-like structures at the Earth's magnetopause.


















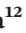


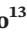




Geophysical Research Letters, 47, e2019GL086726. <https://doi.org/10.1029/2019GL086726>

Received 27 DEC 2019

Accepted 29 FEB 2020

Accepted article online MAR 05 2020

On the Ubiquity of Magnetic Reconnection Inside Flux Transfer Event-Like Structures at the Earth's Magnetopause

N. Fargette¹ , B. Lavraud¹ , M. Øieroset² , T. D. Phan² , S. Toledo-Redondo^{1,3}, R. Kieokaew¹ , C. Jacquey¹ , S. A. Fuselier^{4,5} , K. J. Trattner⁶ , S. Petrinec⁷ , H. Hasegawa⁸ , P. Garnier¹ , V. Génot¹, Q. Lenouvel¹, S. Fadanelli¹, E. Penou¹, J.-A. Sauvaud¹ , D. L. A. Avano⁹ , J. Burch⁴ , M. O. Chandler¹⁰ , V. N. Coffey¹⁰ , J. Dorelli⁹, J. P. Eastwood¹¹ , C. J. Farrugia¹² , D. J. Gershman⁹ , B. L. Giles⁹ , E. Grigorenko¹³, T. E. Moore⁹ , W. R. Paterson⁹ , C. Pollock¹⁴ , Y. Saito⁸ , C. Schiff⁹, and S. E. Smith¹⁵ 

¹Institut de Recherche en Astrophysique et Planétologie, CNRS, UPS, CNES, Université de Toulouse, Toulouse, France, ²Space Sciences Laboratory, University of California, Berkeley, Berkeley, CA, USA, ³Department of Electromagnetism and Electronics, University of Murcia, Murcia, Spain, ⁴Southwest Research Institute, San Antonio, TX, USA, ⁵Department of Physics, University of Texas at San Antonio, San Antonio, TX, USA, ⁶Laboratory for Atmospheric and Space Physics, University of Colorado Boulder, Boulder, CO, USA, ⁷Lockheed Martin Advanced Technology Center, Palo Alto, CA, USA, ⁸Institute of Space and Astronautical Science, JAXA, Sagami-hara, Japan, ⁹NASA Goddard Space Flight Center, Greenbelt, MD, USA, ¹⁰NASA Marshall Space Flight Center, Huntsville, AL, USA, ¹¹The Blackett Laboratory, Department of Physics, Imperial College London, London, UK, ¹²Department of Physics and Space Science Center, University of New Hampshire, Durham, NH, USA, ¹³Space Research Institute of the Russian Academy of Sciences, Moscow, Russia, ¹⁴Denali Scientific, Fairbanks, AK, USA, ¹⁵Department of Physics, Catholic University of America, Washington, DC, USA

Abstract Flux transfer events (FTEs) are transient phenomena frequently observed at the Earth's magnetopause. Their usual interpretation is a flux rope moving away from the reconnection region. However, the Magnetospheric Multiscale Mission revealed that magnetic reconnection sometimes occurs inside these structures, questioning their flux rope configuration. Here we investigate 229 FTE-type structures and find reconnection signatures inside 19% of them. We analyze their large-scale magnetic topology using electron heat flux and find that it is significantly different across the FTE reconnecting current sheets, demonstrating that they are constituted of two magnetically disconnected structures. We also find that the interplanetary magnetic field (IMF) associated with reconnecting FTEs presents a strong B_y component. We discuss several formation mechanisms to explain these observations. In particular, the maximum magnetic shear model predicts that for large IMF B_y , two spatially distinct X lines coexist at the magnetopause. They can generate separate magnetic flux tubes that may become interlaced.

Plain Language Summary The solar wind and the Earth's magnetosphere are two gigantic magnetic structures that collide constantly over our heads, in the near-space environment. At the boundary of their interaction (the magnetopause), the fundamental process of magnetic reconnection can occur. It is there that dynamic magnetic structures called “flux transfer events” are formed. They travel fast along the magnetopause and transport a lot of energy, from the solar wind into the magnetosphere. These structures are yet not well understood, as underlined by the recent observations made by the Magnetospheric Multiscale Mission (MMS), launched in 2015 by National Aeronautics and Space Administration. The four-spacecraft mission, specifically designed to study the physics happening at the magnetopause, is capable of measuring right into these magnetic structures, collecting data on their particles and magnetic field properties. When analyzing MMS data, we found that 19% of the flux transfer events were not constituted of one, but two structures with very different properties. These dual magnetic structures tend to appear when the solar wind's magnetic field is oriented mainly toward the east or the west. From these observations and based on existing models of the magnetopause, we propose a scenario that allows such dual structures to form as interlaced magnetic tubes.

1. Introduction

Flux transfer events (FTEs) are transient phenomena that frequently occur at the Earth's dayside magnetopause, resulting from the dynamic interaction of the solar wind with the magnetosphere. In the early model of Russell and Elphic (1979), they result from bursty and patchy magnetic reconnection and consist in elbow flux tubes moving away from the subsolar region. Two main models were later proposed. The first one (Southwood et al., 1988; Scholer, 1988) is based on a single spatially stable X-line at the subsolar magnetopause, but whose reconnection rate varies over time. This time variation leads to the formation of magnetic field bulges that are identified as FTEs. The other main model is the multiple X-line scenario (Lee & Fu, 1985), relying on two X-lines appearing sequentially on the magnetopause. As the first X-line forms and then drifts toward the poles, a second X-line reforms near the equator (and remains connected to the first one). The FTE is then the structure trapped in between these two reconnection lines. Over the years, many studies have been conducted to discriminate between these formation models through simulations (e.g., Fedder et al., 2002; Raeder, 2006) and multispacecraft observations (e.g., Hasegawa et al., 2006, 2010; Farrugia et al., 2016). The literature to date suggests a paradigm such that the multiple X-line model is the predominant FTE formation mechanism. In all of these views, FTEs resemble flux ropes, as they are thought of as three-dimensional helical structures. Their expected in situ signatures are primarily an enhancement in their core magnetic field strength and a bipolar signature in the magnetic field component normal to the magnetopause surface.

The Magnetospheric Multiscale Mission (MMS, Burch et al., 2016) with its high-resolution instrumentation has unveiled new features of FTEs. In particular, structures that look like classical FTEs have been reported to display reconnection signatures in their center, with clear ion jets correlated with a thin current sheet. While thin current sheets inside FTEs had previously been observed with the Time History of Events and Macroscale Interactions during Substorms (THEMIS) missions (e.g., Hasegawa et al., 2010; Øieroset et al., 2011), only the recent MMS measurements enabled us to confirm that magnetic reconnection was occurring (Øieroset et al., 2019, 2016; Kacem et al., 2018). Detailed studies of such events led to the conclusion that these structures did not match the regular magnetic flux rope configuration, but rather consisted of interlaced flux tubes such that the reconnecting current sheet separates two magnetically disconnected regions (Kacem et al., 2018; Øieroset et al., 2019). The interpretation of some FTE-type phenomena as complex 3-D structures with interlaced flux tubes was first proposed by Nishida (1989) and Hesse et al. (1990). It was studied through simulations (Lee et al., 1993; Otto, 1995; Cardoso et al., 2013; Farinas Perez et al., 2018) and observed in Cluster data (Louarn et al., 2004) prior to MMS.

In this paper we study statistically the FTEs observed by MMS, investigating in more depth the occurrence and implications of the reconnection signatures found inside FTEs. We find that 19% of FTEs present these signatures in their core and are consistent with the magnetically disconnected flux tube structure similar to Kacem et al. (2018). We also find that the interplanetary magnetic field's (IMF's) orientation plays a significant role in the formation of such structures.

2. Data

We use data measured by the four-spacecraft MMS mission throughout phase 1, from 2015 to 2017. The magnetic field data are acquired by the fluxgate magnetometer (Russell et al., 2016), with a 128-Hz time resolution and a 0.1-nT precision. The ion and electron distribution functions and associated moments are acquired by the Fast Plasma Investigation instruments (Pollock et al., 2016). Only burst mode data are used, giving a time resolution of 30 ms for electron measurement and 150 ms for ions. Data are presented in the Geocentric Solar Ecliptic (GSE) coordinate system and taken from the MMS1 spacecraft.

We also obtain solar wind conditions from the OMNI database (King & Papitashvili, 2005).

3. Selection Process

Although our selection process tries to be as objective as possible, part of it relies on data visual inspection and thus is susceptible to subjectivity. For reproducibility purposes, the auxiliary material contains timetables of all selected events.

3.1. FTE Selection

To build the FTE database, we examined all the events listed as potential FTEs and flux ropes by the Scientists In The Loop (SITL) of the MMS mission for Phases 1A and 1B. We discarded events that were eventually not FTEs (e.g., magnetopause crossings, bow shock crossings, or other associated features). We selected the FTEs based on visual inspection of the data, focusing on the following prime signatures:

- an increase in the total and magnetic pressures, and
- a bipolar signature in one of the components of the magnetic field.

This manual selection process was done using data plots in GSE coordinates, and thus there was no a priori requirement as to which component of the magnetic field was showing a bipolar signature suggestive of a flux rope. After this selection process, 229 events remained. The boundaries of the events were defined based on sharp variations in the profiles of magnetic field, ion and electron velocity, densities, and temperatures.

3.2. Reconnection Identification

The criteria used to identify reconnecting current sheets in the core of the structures are as follows:

- an ion jet signature in the ion velocity (in the L component from hybrid minimum variance analysis (MVA) as detailed next). For very sharp current sheets, the electron velocity was also used (higher time resolution);
- a sharp gradient (monotonous or sometimes bifurcated) in the associated L component of the magnetic field;
- a decrease in the magnetic field strength owing to energy conversion;
- an increase in electron temperature; and
- an increase in density.

All signatures were not necessarily required at the exact same time for all events. The importance of the last three signatures in particular varies with parameters such as plasma β and asymmetries across the current sheet. In order to best identify the reconnection signatures in the magnetic field and velocity, we determined the current sheet LMN coordinate system through a hybrid MVA (Gosling & Phan, 2013). The current sheet normal is given by $\mathbf{N} = \frac{\mathbf{B}_1 \wedge \mathbf{B}_2}{|\mathbf{B}_1 \wedge \mathbf{B}_2|}$ where \mathbf{B}_1 and \mathbf{B}_2 are the asymptotic magnetic fields across the current sheet; $\mathbf{M} = \mathbf{L}' \wedge \mathbf{N}$ where \mathbf{L}' is the direction of maximum variance of the magnetic field obtained from straight application of MVA (Sonnerup & Cahill, 1967); finally, $\mathbf{L} = \mathbf{N} \wedge \mathbf{M}$ completes the orthogonal frame.

In the supporting information of this paper we provide a test of the Swisdak et al. (2003) condition for magnetic reconnection. We compare the magnetic shear angle to the difference in plasma β across the current sheets, as done by Phan et al. (2010, 2013). Our results are consistent with magnetic reconnection occurring inside these events, further confirming our selection of these cases as “reconnecting FTEs” (cf. Text S1 in the supporting information).

3.3. Event Illustration

Two time intervals are now described as representative of the types of events we distinguish in this work. The first one is a standard flux rope-type FTE at the magnetopause (12 November 2015, 07 hr 20:20–07 hr 20:34), and the second one presents a strong reconnection signature at its center (2015/10/31, 07 h18:00–07 h19:15). The latter was studied in more depth by Øieroset et al. (2016), who provided evidence of magnetic reconnection using both observations and simulations. Figure 1 presents MMS1 data for both events, with slightly larger time intervals.

In the first event (Figures 1a–1h), the total pressure is dominated by the plasma thermal pressure except in the core of the event where magnetic pressure dominates and total pressure enhances. The magnetic field variation is smooth and presents a bipolar signature in B_x . Density and magnetic field (Figures 1e and 1b) indicate that the event takes place in the magnetosheath. There are no striking features to note in ion velocity, electron velocity, or electron parallel temperature. In the pitch angle distribution (PAD) of suprathermal electrons (~ 250 –700 eV, Figure 1h), large fluxes can be noted at 90° at the beginning and end of the event. They correspond to local minima in the magnetic field strength (Figure 1b), which suggests that these are local magnetic bottle configurations leading to local particle trapping.

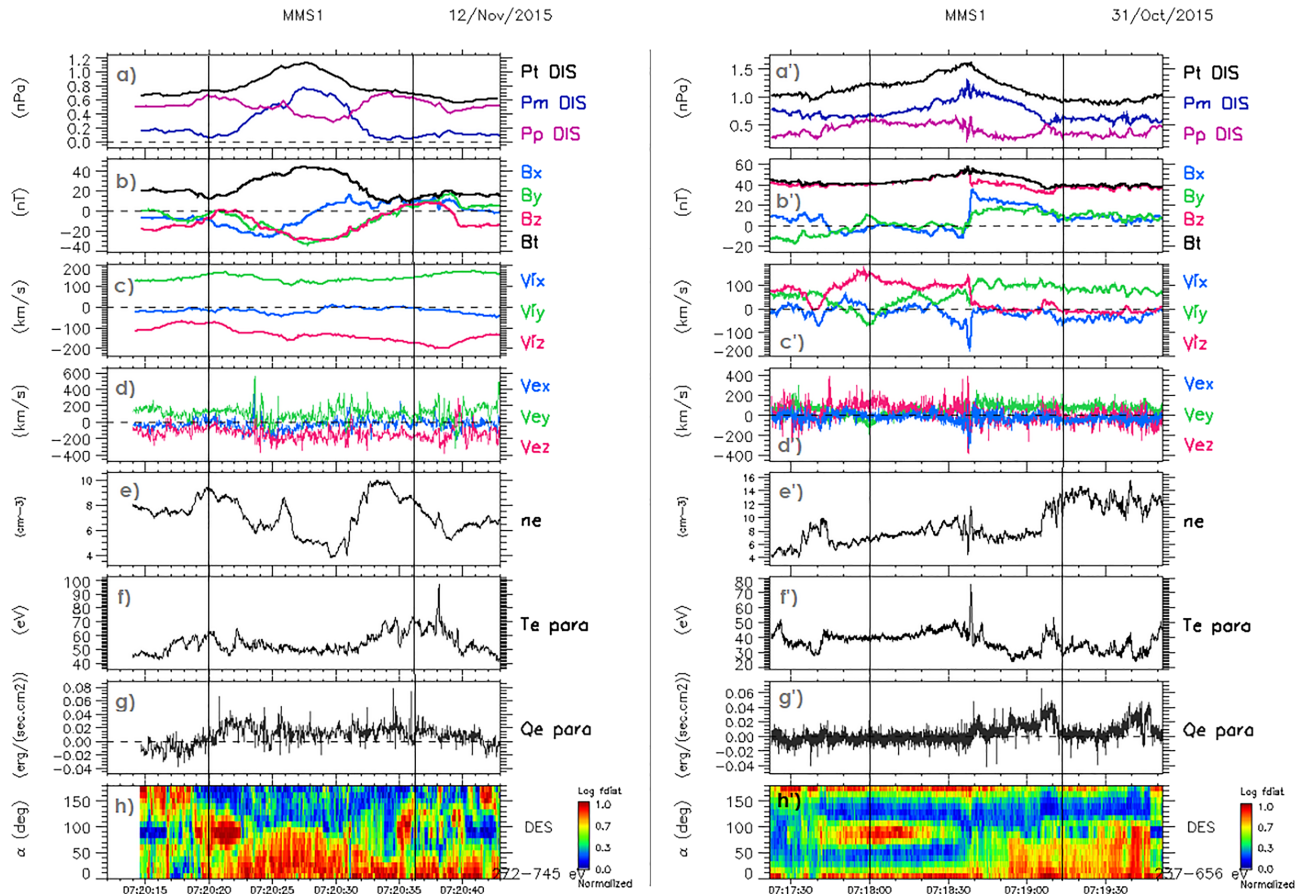


Figure 1. Illustration of the two types of FTE-like structures observed by MMS, boundaries shown as black vertical lines. (left) Standard flux rope event from 12 November 2015, 07 hr20:20–07 hr20:34; (right) Event with core reconnection from 31 October 2015, 07 hr18:00–07 hr19:15. From top to bottom, the panels present (a) the total, magnetic, and particle thermal pressure P_t , P_m , and P_p , respectively; (b) the magnetic field (GSE); (c) the ion velocity (GSE); (d) the electron velocity (GSE); (e) the electron density, (f) the electron parallel temperature; (g) the electron parallel heat flux, and (h) the electron pitch angle distribution (250–700 eV).

The second event (Figures 1a'–1h') also shows a core enhancement in total pressure (albeit being dominated by magnetic pressure throughout) and a bipolar variation in the B_x component. In contrast with the previous event, the variation is sharp and consistent with a localized thin current sheet at the center of the structure. Concomitant with this current sheet, the ion velocity (Figure 1c') displays a jet at 07 hr18:38 s with a V_{ix} spike around -150 km/s. A coincident electron jet (Figure 1d') with $V_{ex} \sim -280$ km/s is also observed, together with an increase in electron parallel temperature (Figure 1f') from 40 to 75 eV. All these signatures are consistent with magnetic reconnection occurring at this thin current sheet in the core of the event. Finally, PADs (Figure 1h') are drastically different on each side, with combined populations of bidirectional (0° and 180° PA) and trapped electrons (90° PA) before the current sheet, but a much broader and mostly field-aligned PAD after it.

In total, 43 events are identified as FTE-like structures with core magnetic reconnection. They amount to 19% of the overall FTE database.

4. Results

In this section we first focus on the spatial variations of the properties of the parallel heat fluxes and associated PAD of suprathermal electrons inside FTE-like structures. We then investigate the solar wind conditions that prevail just prior to the observed FTEs and may control their formation.

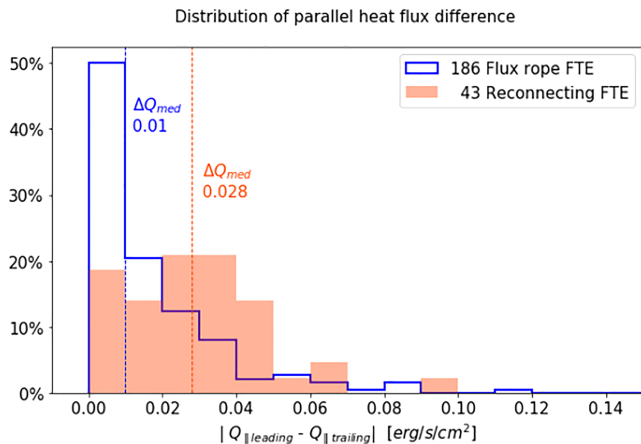


Figure 2. Parallel electron heat flux variation's distribution within the FTEs. The $\Delta Q_{||}$ percentage distribution is plotted for flux rope FTEs and reconnecting FTEs. The dotted lines are placed at the median value. In order to better zoom on the core of the distributions, one outlier point does not appear in the reconnecting FTE plots ($\Delta Q_{||} = 0.33$ erg/s/cm²).

expects that regular flux ropes should have roughly the same $Q_{||}$ throughout the event, while reconnecting FTEs should statistically show a much larger difference in $Q_{||}$ across the reconnecting current sheet. To assess the possibility of such a difference we used the following method:

- For reconnecting FTEs, the time average of $Q_{||}$ is computed before (leading part) and after (trailing part) the identified reconnection jet and within the FTE's bounds.
- For regular FTEs, the time average of $Q_{||}$ is computed before and after the center of the flux rope, where the magnetic field strength is maximum.

For each event, the scalar $\Delta Q_{||} = |Q_{||\text{leading}} - Q_{||\text{trailing}}|$ was computed, and its distribution is represented in Figure 2. The bins are 0.01 erg/s/cm² wide, and the ordinate is the percentage of events in each bin. When comparing both distributions, we observe that the median for the regular flux rope is 0.010 erg/s/cm² versus 0.028 erg/s/cm² for the reconnecting FTEs. The standard deviations also vary from $\sigma = 0.019$ erg/s/cm² (flux ropes) to $\sigma = 0.050$ erg/s/cm² (reconnecting FTEs). This result shows that the heat flux typically changes more between the leading and trailing segments of the structure when a reconnecting current sheet is identified inside the event. We also observe that some reconnecting FTEs have similar heat fluxes between their leading and trailing parts (e.g., first two bins in Figure 2). First, we note that the suprathermal PAD properties can be different despite a similar heat flux, which is an integral quantity. Even if the PADs were similar, it does not preclude the two flux tubes to be connected to different regions despite the electron source properties being similar.

4.2. Solar Wind Conditions

We compared the distribution of the solar wind parameters during the time preceding FTEs to their standard distribution. Data from OMNI were averaged over 15 min before each FTE to yield the solar wind parameters most likely associated with its formation. Consistency of the results was checked by averaging over different time intervals from 5 to 25 min, and the results remained similar.

The orbital data show that FTE locations are distributed uniformly along the equator and follow the Shue et al. (1997) magnetopause model. The positions of flux rope and reconnecting FTEs do not display major differences (cf. Text S2).

Among the solar wind parameters studied, the IMF clock angle $\theta = \tan^{-1}(B_y/B_z)$ stands out as its distribution before FTEs is very different from the standard one. Figure 3 presents the IMF clock angle distributions. Panel (a) serves as a control sample and shows the distribution throughout the whole period of observation. The radial scale is the number of solar wind measurements counted in one bin (22.5° each). This oval distribution extended in the Y_{GSE} direction is expected as the result of the preferential Parker spiral orientation of

4.1. Quantification of Changes in Connectivity

Suprathermal electrons (300–700 eV) move essentially freely along magnetic field lines and are thus good tracers of magnetic topology. Accordingly, their PAD along a given field line should not change much. If density and magnetic field variations may induce changes in the absolute value of the flux, or the width of the field-aligned/anti-field-aligned peaks, the basic structure of the PAD should persist. For instance, in Figure 1g the PAD throughout the event is essentially always field aligned with some broadening occurring with magnetic field strength enhancement toward the core of the FTE. By contrast, in Figure 1g' the PADs across the reconnecting current sheet are vastly different (cf. section 3.3). These distinct regions are therefore not magnetically connected to each other.

A visual inspection of the PADs was conducted for reconnecting FTEs. They seemed to be different on each side of the identified reconnection exhaust similarly to Figure 1g'. To quantify this discrepancy, we analyzed the parallel electron heat flux $Q_{||}$, which yields information on the asymmetries in the tail of the electron population (e.g., Lavraud et al., 2006, who use both PAD spectrograms and heat fluxes as done here). One

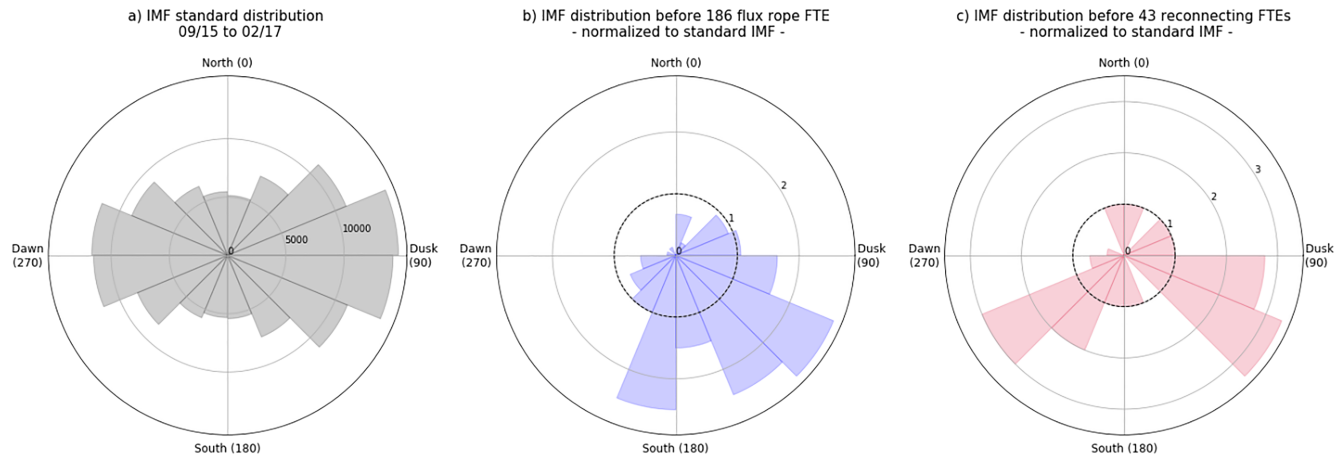


Figure 3. IMF clock angle distributions, bins are 22.5° wide. (a) Count distribution for the total period of observation from September 2015 to February 2017; (b) distribution for standard flux rope FTEs normalized to panel (a); (c) distribution for reconnecting FTEs normalized to panel (a). The dashed line in panels (b) and (c) represents the reference of the standard IMF (unit value). A distribution similar to the IMF would be isotropic and equal to 1 when normalized. Compare with text for more details.

the IMF in the ecliptic plane (e.g., Kivelson & Russell, 1995). Panels (b) and (c) respectively present the IMF clock angle normalized distributions for flux rope and reconnecting FTEs. They are normalized to the standard IMF distribution of panel (a) to better quantify actual trends: We represent the percentage of events observed in one bin, divided by the percentage of solar wind measurements in the same bin. A distribution similar to standard IMF should be isotropic and equal to 1 (thick black dashed circle).

A first clear trend is that the IMF is mostly directed southward before the FTE observations. This agrees with previous studies on the clock angle influence on FTE occurrence (e.g., Russell et al., 1985; Fear et al., 2012) and is consistent with the role of magnetic reconnection in the formation of FTEs (Russell & Elphic, 1979; Raeder, 2006). A second trend is that the distribution for regular flux rope FTEs (Figure 3b) shows a significant duskward component. Of particular interest here is the strongly marked tendency for large B_y in the case of FTEs with reconnecting current sheets (Figure 3c), with a much smaller occurrence for purely southward IMF. Over the complete set of events, 150 fall into bins with large B_y values ($[45-135]^\circ$; $[225-315]^\circ$). Among these 150 events with large B_y , 37 (25%) are reconnecting FTEs.

5. Discussion

The first main and unexpected result of this study is the fact that magnetic reconnection occurs frequently inside FTE-type structures. Out of 229 events, 43 show signatures of magnetic reconnection within their core, amounting to 19%. Such signatures are not expected in regular FTEs.

Øieroset et al. (2016) noted that field lines originating from two X-lines could compress a current sheet and cause reconnection in the center of the FTE. Kacem et al. (2018) found that the PAD across the compressed current sheet are drastically different for suprathermal electrons. This observation is inconsistent with the connectivity implied by a three-dimensional helical magnetic field, and rather indicates that the two sides of the structure are not magnetically connected. Kacem et al. (2018) suggested that the 3-D interaction of magnetic field lines originated from two X-lines forms interlaced flux tubes (akin to the model by Nishida, 1989; Hesse et al., 1990) that resemble an FTE.

For the majority of the reconnecting cases studied here, the leading and trailing parts of the structures seem disconnected (Figure 2). We thus find that the events with a reconnecting current sheet have PADs and heat flux properties statistically consistent with this model of interlaced flux tubes. The fact that they are slightly longer than regular flux ropes is also consistent with them being two structures rather than one (cf. Text S3). We also found that the IMF displays a very strong B_y component just prior to the observation of reconnecting FTEs (section 4.2). Based on all these facts and recent literature, we now discuss several possible interpretations.

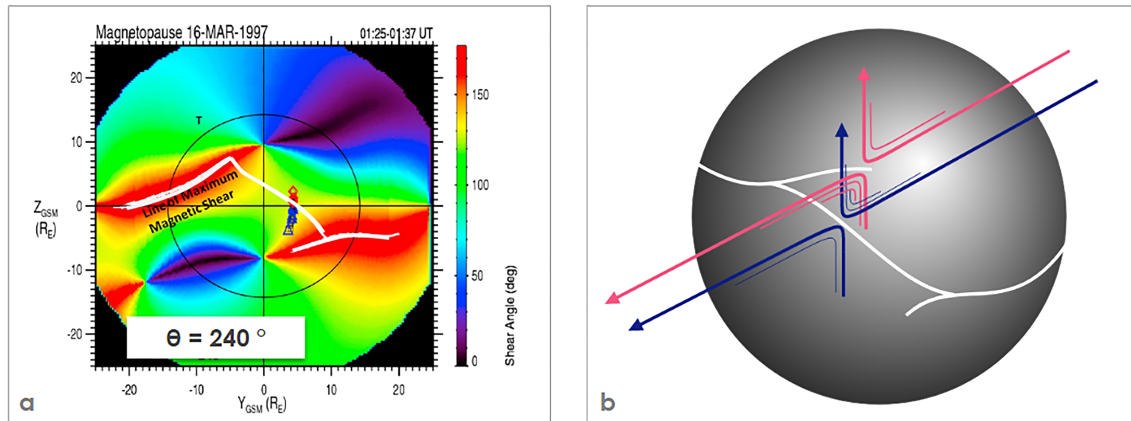


Figure 4. Proposition of a configuration for the formation of interlaced flux tube FTEs, based on a bifurcation of the X-line at the dayside magnetopause for large IMF B_y . (a) Magnetic shear angle between the IMF (240°) and the magnetosphere in the (Y_{GSM}/Z_{GSM}) plane, from Trattner et al. (2012). (b) Schematic showing in white a bifurcated reconnection line on the Earth's magnetopause for such a clock angle. In blue and red, we show field lines produced by two distinct reconnection sites and whose geometry is proposed to generate interlaced flux tubes.

First, the influence of the IMF B_y on the occurrence of interlaced flux tubes was investigated through simulation by Cardoso et al. (2013) and more recently by Farinas Perez et al. (2018). When imposing a strong B_y component on the IMF together with a southward B_z , they observed the formation of two “interlinked” flux tubes (called IFT) out of five FTE-type structures generated in the simulation. They identified two distinct formation processes for each event. For one, the strong B_y component of the IMF leads to the formation of two reconnection sites, respectively, northward and southward of the equator. This is explained as a consequence of resistive tearing instability at the subsolar point. Both reconnection sites then generate distinct sets of flux tubes with different connectivity, that interlace and form what resembles an FTE in a fashion very similar to the scenario described in Kacem et al. (2018). By contrast, their second event is shown to originate as a standard flux rope FTE. It evolves afterward into an interlinked flux tube structure with different connectivity as well, but through processes that remain to be explained.

Another formation mechanism is now proposed. It is based on the known effect of the IMF B_y component on dayside X-line geometry and location as studied by, for example, Trattner et al. (2007, 2012) and Petrinec et al. (2014). The maximum magnetic shear model (Trattner et al., 2007) determines that for a B_y -dominated IMF the X-line could be “bifurcated” in some specific locations on the magnetopause, as displayed in the left panel of Figure 4 (from Trattner et al., 2012). It shows, for a given event unrelated to the present study (this figure is merely used here for illustrative purpose), the magnetic shear angle across the magnetopause projected into the Y-Z plane. The IMF clock angle in this case is of 240° . The white lines represent the X-line location related to the maximum magnetic shear angle location.

We note that this model allows for the existence of two coincidental X-lines at the same longitude. As shown with the blue and red field lines in Figure 4b, we propose that such a configuration may lead to the formation of complex structures such as interlaced flux tubes. Importantly, we note that unlike the sequential X-line model, which is based on successive X-line formation (temporally), the present model does not require sequential X-line formation. Under large B_y IMF, various regions at the magnetopause feature large magnetic shears and, therefore, are good candidates to initiate reconnection and sustain an X line. This may allow simultaneous coexistence of multiple X lines and facilitate interlacing between flux tubes. This is thus largely different from the regular sequential X-line model for FTE formation that may lead to the formation of regular flux rope FTEs.

6. Conclusion

We have studied FTE-like structures observed by the MMS mission throughout Phase 1, with particular emphasis on the occurrence of magnetic reconnection inside these structures. We find that magnetic

reconnection occurs inside 19% of them (43/229 events), with events looking like FTEs but inconsistent with their classical description as they present a marked current sheet in their core.

We analyzed the parallel electron heat flux inside FTEs as it is a good tracer of magnetic connectivity. We find that the variation in Q_{\parallel} across the current sheet of reconnecting FTEs is significantly larger (Median(ΔQ_{\parallel}) = 0.028 erg/s/cm²) than throughout regular flux rope FTEs (Median(ΔQ_{\parallel}) = 0.010 erg/s/cm²). This is statistically consistent with reconnecting FTEs being constituted of regions magnetically disconnected from each other.

We investigated solar wind conditions prior to the observed FTEs. While most other parameters essentially remain unchanged, the IMF clock angle distribution is found to be directed mainly southward and duskward for regular FTEs while it has a much stronger B_y component in the case of events with a reconnecting current sheet.

Our statistical analysis thus supports the recent work by Kacem et al. (2018) and Øieroset et al. (2019), where FTE-like structures are described as interlaced flux tubes. We further discuss the link between a prevailing large IMF B_y component in the solar wind and the formation of such structures. Two mechanisms were proposed by Farinas Perez et al. (2018) on the basis of simulation and suggest that interlaced flux tubes may form either through resistive tearing instability developing at the subsolar point or through the evolution of a regular FTE into a more complex 3-D structure. We propose an additional formation mechanism based on the maximum magnetic shear angle model at the magnetopause (Trattner et al., 2007), which can create bifurcated X-lines at the dayside magnetopause for large IMF B_y . It can lead to the interlacing of flux tubes from two spatially distinct X-lines at the same longitude. This mechanism is drastically different from the most studied FTE formation mechanism based on temporally sequential reconnection (Raeder, 2006) that could still form regular nonreconnecting FTEs. These various scenarios remain to be tested in future studies.

Acknowledgments

MMS data are available from this site (<https://lasp.colorado.edu/mms/sdc/public/>). We visualize data using the CLWeb software available at <http://clweb.irap.omp.eu/>, developed by E. Penou. Work at IRAP was supported by CNRS, CNES, and UPS. S. T. R. acknowledges support of the Ministry of Economy and Competitiveness (MINECO) of Spain, Research Project FIS2017-90102-R. This research was supported by NASA Grants NNX17AE12G and 80NSSC18K1380 at UC Berkeley.

References

- Burch, J. L., Moore, T. E., Torbert, R. B., & Giles, B. L. (2016). Magnetospheric multiscale overview and science objectives. *Space Science Review*, 199(1–4), 5–21. <https://doi.org/10.1007/s11214-015-0164-9>
- Cardoso, R., Gonzalez, W. D., Sibeck, D. G., Kuznetsova, M., & Koga, D. (2013). Magnetopause reconnection and interlinked flux tubes. *Annales Geophysicae*, 31(10), 1853–1866. <https://doi.org/10.5194/angeo-31-1853-2013>
- Farinas Perez, G., Cardoso, F. R., Sibeck, D., Gonzalez, W. D., Fackskó, G., Coxon, J. C., & Pembroke, A. D. (2018). Generation mechanism for interlinked flux tubes on the magnetopause. *Journal of Geophysical Research: Space Physics*, 123, 1337–1355. <https://doi.org/10.1002/2017JA024664>
- Farrugia, J., Lavraud, B., Torbert, R. B., Argall, M., Kacem, I., Yu, W., et al. (2016). Magnetospheric Multiscale Mission observations and non-force free modeling of a flux transfer event immersed in a super-Alfvénic flow. *Geophysical Research Letters*, 43, 6070–6077. <https://doi.org/10.1002/2016GL068758>
- Fear, R. C., Palmroth, M., & Milan, S. E. (2012). Seasonal and clock angle control of the location of flux transfer event signatures at the magnetopause. *Journal of Geophysical Research*, 117, A04202. <https://doi.org/10.1029/2011JA017235>
- Fedder, A., Slinker S. P., Lyon J. G., Russell C. T. (2002). Flux transfer events in global numerical simulations of the magnetosphere. *Journal of Geophysical Research* 107(A5), 1048. <https://doi.org/10.1029/2001JA000025>
- Gosling, J. T., & Phan, T. D. (2013). Magnetic reconnection in the solar wind at current sheets associated with extremely small field shear angles. *Astrophysical Journal Letters*, 763(2), L39. <https://doi.org/10.1088/2041-8205/763/2/L39>
- Hasegawa, B. U., Sonnerup, Ö., Owen, C. J., Klecker, B., Paschmann, G., Balogh, A., & Rème, H. (2006). The structure of flux transfer events recovered from Cluster data. *Annales Geophysicae*, 24(2), 603–618. <https://doi.org/10.5194/angeo-24-603-2006>
- Hasegawa, H., Wang, J., Dunlop, M. W., Pu, Z. Y., Zhang, Q. H., Lavraud, B., et al. (2010). Evidence for a flux transfer event generated by multiple X-line reconnection at the magnetopause. *Geophysical Research Letter*, 37, L16101. <https://doi.org/10.1029/2010GL044219>
- Hesse, M., Birn, J., & Schindler, K. (1990). On the topology of flux transfer events. *Journal of Geophysical Research*, 95(A5), 6549–6560. <https://doi.org/10.1029/JA095iA05p06549>
- Kacem, I., Jacquy, C., Génot, V., Lavraud, B., Vernisse, Y., Marchaudon, A., et al. (2018). Magnetic reconnection at a thin current sheet separating two interlaced flux tubes at the Earth's magnetopause. *Journal of Geophysical Research: Space Physics*, 123, 1779–1793. <https://doi.org/10.1002/2017JA024537>
- King, J. H., & Papitashvili, N. E. (2005). Solar wind spatial scales in and comparisons of hourly Wind and ACE plasma and magnetic field data. *Journal of Geophysical Research*, 110, A02104. <https://doi.org/10.1029/2004JA010649>
- Kivelson, M. G. & Christopher T. Russell (1995). *Introduction to space physics*. Cambridge: Cambridge University Press.
- Lavraud, B., Thomsen, M. F., Lefebvre, B., Schwartz, S. J., Seki, K., Phan, T. D., et al. (2006). Evidence for newly closed magnetosheath field lines at the dayside magnetopause under northward IMF. *Journal of Geophysical Research*, 111, A05211. <https://doi.org/10.1029/2005JA011266>
- Lee, L. C., & Fu, Z. F. (1985). A theory of magnetic flux transfer at the Earth's magnetopause. *Geophysical Research Letter*, 12, 105–108. <https://doi.org/10.1029/GL012i002p00105>
- Lee, L. C., Ma, Z., Fu, Z. F. & Otto, A. (1993). Topology of magnetic flux ropes and formation of fossil flux transfer events and boundary layer plasmas. *Journal of Geophysical Research*, 98(A3), 3943–3952. <https://doi.org/10.1029/92JA02203>
- Louarn, P., Fedorov, A., Budnik, E., Fruit, G., Sauvaud, J. A., Harvey, C. C., et al. (2004). Cluster observations of complex 3D magnetic structures at the magnetopause. *Geophysical Research Letters*, 31, L19805. <https://doi.org/10.1029/2004GL020625>

- Nishida, A. (1989). Can random reconnection on the magnetopause produce the low latitude boundary layer? *Geophysical Research Letters*, *16*(3), 227–230. <https://doi.org/10.1029/GL016i003p00227>
- Øieroset, M., Phan, T. D., Drake, J. F., Eastwood, J. P., Fuselier, S. A., Strangeway, R. J., et al. (2019). Reconnection with magnetic flux pileup at the interface of converging jets at the magnetopause. *Geophysical Research Letter*, *46*, 1937–1946. <https://doi.org/10.1029/2018GL080994>
- Øieroset, M., Phan, T. D., Eastwood, J. P., Fujimoto, M., Daughton, W., Shay, M. A., et al. (2011). Direct evidence for a three-dimensional magnetic flux rope flanked by two active magnetic reconnection X lines at Earth's magnetopause. *Physical Review Letters*, *107*, 165007. <https://doi.org/10.1103/PhysRevLett.107.165007>
- Øieroset, M., Phan, T. D., Haggerty, C., Shay, M. A., Eastwood, J. P., Gershman, D. J., et al. (2016). MMS observations of large guide field symmetric reconnection between colliding reconnection jets at the center of a magnetic flux rope at the magnetopause. *Geophysical Research Letter*, *43*, 5536–5544. <https://doi.org/10.1002/2016GL069166>
- Otto, A. (1995). Forced three-dimensional magnetic reconnection due to linkage of magnetic fluxtubes. *Journal of Geophysical Research*, *100*(A7), 11,863–11,874. <https://doi.org/10.1029/94JA03341>
- Petrinec, S. M., Trattner, K. J., Fuselier, S. A., & Stovall, J. (2014). The steepness of the magnetic shear angle “saddle”: A parameter for con-straining the location of dayside magnetic reconnection? *Journal of Geophysical Research: Space Physics*, *119*, 8404–8414. <https://doi.org/10.1002/2014JA020209>
- Phan, T. D., Gosling, J. T., Paschmann, G., Pasma, C., Drake, J. F., Øieroset, M., et al. (2010). The dependence of magnetic reconnection on plasma β and magnetic shear: Evidence from solar wind observations. *Astrophysical Journal Letters*, *719*(2), L199–L203. <https://doi.org/10.1088/2041-8205/719/2/L199>
- Phan, T. D., Paschmann, G., Gosling, J. T., Øieroset, M., Fujimoto, M., Drake, J. F., & Angelopoulos, V. (2013). The dependence of magnetic reconnection on plasma β and magnetic shear: Evidence from magnetopause observations. *Geophysical Research Letters*, *40*, 11–16. <https://doi.org/10.1029/2012GL054528>
- Pollock, C., Moore, T., Jacques, A., Burch, J., Gliese, U., Saito, Y., et al. (2016). Fast plasma investigation for magnetospheric multiscale. *Space Science Review*, *199*(1–4), 331–406. <https://doi.org/10.1007/s11214-016-0245-4>
- Raeder, J. (2006). Flux transfer events: 1. Generation mechanism for strong southward IMF. *Annales Geophysicae*, *24*(1), 381–392. <https://doi.org/10.5194/angeo-24-381-2006>
- Russell, C. T., Anderson, B. J., Baumjohann, W., Bromund, K. R., Dearborn, D., Fischer, D., et al. (2016). The magnetospheric multiscale magnetometers. *Space Science Review*, *199*(1–4), 189–256. <https://doi.org/10.1007/s11214-014-0057-3>
- Russell, C. T., Berchem, J., & Luhmann, J. G. (1985). On the source region of flux transfer events. *Advances in Space Research*, *5*(4), 363–368. [https://doi.org/10.1016/0273-1177\(85\)90162-0](https://doi.org/10.1016/0273-1177(85)90162-0)
- Russell, C. T., & Elphic, R. C. (1979). ISEE observations of flux transfer events at the dayside magnetopause. *Geophysical Research Letter*, *6*(1), 33–36. <https://doi.org/10.1029/GL006i001p00033>
- Scholer, M. (1988). Magnetic flux transfer at the magnetopause based on single X line bursty re-connection. *Geophysical Research Letter*, *15*(4), 291–294. <https://doi.org/10.1029/GL015i004p00291>
- Shue, J. -H., Chao, J. K., Fu, H. C., Russell, C. T., Song, P., Khurana, K. K., & Singer, H. J. (1997). A new functional form to study the solar wind control of the magnetopause size and shape. *Journal of Geophysical Research*, *102*(A5), 9497–9512. <https://doi.org/10.1029/97JA00196>
- Sonnerup, B. U. Ö., & Cahill Jr, L. J. (1967). Magnetopause structure and attitude from Explorer 12 observations. *Journal of Geophysical Research*, *72*, 171–183. <https://doi.org/10.1029/JZ072i001p00171>
- Southwood, D. J., Farrugia, C. J., & Saunders, M. A. (1988). What are flux transfer events? *Planetary and Space Science*, *36*(5), 503–508. [https://doi.org/10.1016/0032-0633\(88\)90109-2](https://doi.org/10.1016/0032-0633(88)90109-2)
- Swisdak, M., Rogers, B. N., Drake, J. F., & Shay, M. A. (2003). Diamagnetic suppression of component magnetic reconnection at the magnetopause. *Journal of Geophysical Research*, *108*(A5), 1218. <https://doi.org/10.1029/2002JA009726>
- Trattner, K. J., Mulcock, J. S., Petrinec, S. M., & Fuselier, S. A. (2007). Probing the boundary between antiparallel and component reconnection during southward interplanetary magnetic field conditions. *Journal of Geophysical Research*, *112*, A08210. <https://doi.org/10.1029/2007JA012270>
- Trattner, K. J., Petrinec, S. M., Fuselier, S. A., Omid, N., & Sibeck, D. G. (2012). Evidence of multiple reconnection lines at the magnetopause from cusp observations. *Journal of Geophysical Research*, *117*, A01213. <https://doi.org/10.1029/2011JA017080>